Euphytica **98:** 1–10, 1997.

Influence of cytoplasmic-nuclear male sterility systems on microsporogenesis in pearl millet (*Pennisetum glaucum* (L.) R. Br.)

A.K. Chhabra[1]*, I.S. Khairwal[1], K.N. Rai[2], C.T. Hash[2] & A.K. Murthy[3]
[1] *Department of Plant Breeding, CCS Haryana Agricultural University, Hisar 125 004, Haryana, India;* [2] *Genetic Enhancement Division and* [3] *Crop Protection Division, ICRISAT Asia Center, Patancheru P.O. 502 324, Andhra Pradesh, India; (* address for correspondence: RDS 23, Old Campus, CCS Haryana Agricultural University, Hisar 125 004, Haryana, India)*

Received 30 December 1996; accepted 25 June 1997

Key words: cytoplasmic-nuclear male sterility, isonuclear lines, microsporogenesis, pearl millet, *Pennisetum glaucum*, pollen degeneration

Summary

Influence of a range of cytoplasms on microsporogenesis and anther development in pearl millet was studied using six isonuclear A-lines having five cytoplasms (A_1, A_2, A_3, A_4 and A_v) and the nuclear genome of 81B. 81B was used as a male-fertile control. Microsporogenesis and anther development were normal in 81B. However, pollen mother cell (PMC)/microspore/pollen degeneration in the six A-lines occurred at different stages of anther development. Each cytoplasm had its unique influence on microsporogenesis and anther development as evidenced by different developmental paths followed by them leading to pollen abortion. The cause of pollen abortion differed from line to line, from floret to floret within a spikelet, from anther to anther within a floret, and in some cases even from locule to locule within an anther. Events that led to male sterility included anomalies in tapetum and callose behaviour, persistence of tapetum, endothecium thickness, and other unknown causes. The present study also indicated that anther/pollen development was more irregular in Pb $406A_3$. In $81A_4$ and $81A_1$ > 95% of anther locules followed a definite developmental path to pollen abortion. In the other A-lines many developmental paths were observed within the line and pollen degeneration occurred at various stages. This could be one of the reasons for greater instability of male sterility in the A_2 and A_3 systems and greater stability of male sterility in the A_1 and A_4 systems.

Abbreviations: CDS – cool dry season, HDS – hot dry season, CMS – cytoplasmic-nuclear male sterility, ITS – intra tapetal syncytium, PMC – pollen mother cell

Introduction

Past research has identified several distinct systems of cytoplasmic-nuclear male sterility (CMS) in pearl millet, *Pennisetum glaucum* (L.) R. Br. (Burton & Athwal, 1967; Appadurai et al., 1982; Aken'Ova, 1985; Marchais & Pernes, 1985; Hanna, 1989; Sujata et al., 1994; Rai, 1995). Fertility/sterility patterns of hybrids (Burton & Athwal, 1967; Appadurai et al., 1982; Aken'Ova, 1985; Marchais & Pernes, 1985; Rai & Hash, 1990; Rai, 1995) and mitochondrial DNA-RFLP patterns (Smith et al., 1987; Smith & Chowdhury, 1989, 1991; Sivaramakrishnan et al., 1993; Rajeshwari et al., 1994; Sujata et al., 1994; Chhabra, 1995) have been used to characterize these CMS sources. Microsporogenesis pattern has also been used to characterize CMS differences in maize (Lee et al., 1979, 1980). Pearl millet studies of A_1-system CMS lines show strong effect of the genetic background on microsporogenesis. For example, Burton (1958) indicated that microsporogenesis breakdown occurs mainly during tetrad formation. In other material, meiosis proceeds normally but microspores degenerate immediately after their release (Singh & Sharma, 1963; Balarami Reddy & Reddi,

1974; Sharma, 1978). In all the cases the tapetum persisted in male-sterile lines near anther maturity except in male-sterile line 628A studied by Balarami Reddy & Reddi (1974). In CMS line 628A, its maintainer 628B and male-fertile Tift 23B, the tapetum degenerated completely towards anther dehiscence (Balarami Reddy & Reddi, 1974). Male sterility was also associated with a thicker endothecium in 628A and Tift 23A (Balarami Reddy & Reddi, 1974). These A-lines had a thin endothecium initially but it increased in thickness as pollen matured, while this was reversed in their B-lines. The anther epidermis of pollen shedders was thicker compared to pure Tift 23A or Tift 23B and endothecium thickness was intermediate to the endothecium thickness in Tift 23A and Tift 23B.

Microsporogenesis has not been previously studied in pearl millet CMS systems other than A_1. To determine precisely the effect of various CMS systems on microsporogenesis, isonuclear CMS lines in the genetic background of one or more universal maintainers would be the ideal material. A number of near-isonuclear CMS lines based on some of these CMS systems have been assembled at ICRISAT Asia Center (IAC). We have used isonuclear lines in the background of 81B to study anther development in male-sterile and male-fertile lines to determine precisely the stage and possible cause of pollen abortion in a range of pearl millet CMS systems.

Materials and methods

The six isonuclear A-lines, based on the nuclear genome of 81B, included in this study were $81A_1$ with Tift $23DA_1$ cytoplasm (Anand Kumar et al., 1984), ICMA 88001 = $81A_v$, with *violaceum* cytoplasm (Marchais & Pernes, 1985), $81A_4$ = $81A_4$ with *monodii* = *violaceum* cytoplasm (Hanna, 1989), Pb $310A_2$ and Pb $311A_2$ (A_2 cytoplasm via two different accessions), and A_3 CMS line, Pb $406A_3$ (Virk & Mangat, 1987, 1988, 1989; Virk et al., 1990). Male-fertile line 81B (control), the common maintainer of all these A-lines was also included in this study.

The material was grown in the polyhouse in the cool dry season (CDS) and the hot dry season (HDS) of 1993/94 at ICRISAT Asia Center (IAC). Microsporogenesis was studied in both seasons. Spikelets were collected and fixed in a freshly prepared Carnoy's fluid (6 absolute alcohol : 3 glacial acetic acid : 1 chloroform) in which a few drops of ferric chloride (mordant) were added @ 1 ml of saturated aqueous solution of ferric chloride to 200 ml of Carnoy's fluid. The material was transferred to fresh fixative after 1–2 h and stored at 4 °C. Florets/spikelets for histological studies were collected at various stages of anther development as defined in Figure 1. These stages were defined based on anther development in 81B. Corresponding developmental stages were studied in male-sterile lines. For each stage 50 to 60 florets from 10–15 panicles were examined in each line.

Florets were collected and fixed in 3% glutaraldehyde in 0.1 M phosphate buffer (pH 7.2), gently vacuum infiltrated and washed four times in 0.1 M sodium phosphate buffer (pH 7.2) over a period of 2 h. Postfixation was in 2% aqueous osmium tetroxide for 4 h. Samples were dehydrated in a graded series of acetone and embedded in Spurr epoxy resin (Spurr, 1969). Transverse sections of entire florets/spikelets were cut to a thickness of 5–8 μm with a glass knife using an Ultracut Reichert Jung ultra-microtome and stained with LADD Multiple stain (LADD # 70955) and 0.5% malachite green. Samples were then washed thoroughly with water and gently dried and mounted using Permount (Fisher). Samples were examined under a light microscope (Olympus BH2 System) and photographed using Kodak 100 ASA B/W films.

Results and discussion

Anther development and microsporogenesis in male-fertile line 81B

Microsporogenesis and anther development in all isonuclear lines was consistent over seasons. Histological studies at successive developmental stages revealed that anther development and microsporogenesis followed a normal course in male-fertile line 81B. All the anthers studied followed the same developmental pattern (Figure 1). Prior to initiation of meiosis, young anthers contained sporogenous tissue surrounded by tapetum, followed by a middle layer, an endothecium and the epidermis (Figure 2A). Callose deposition started at the locule center only after this stage, and became conspicuous at the onset of meiosis (Figure 2B). Tapetum thickness continued to increase and the central callose splitted along the sporocyte walls (Figure 2C). Following this, the sporocytes migrated towards the inner tapetal wall carrying callose tips on their inner face. This event occurred concurrently in all the locules of an anther (Figure 2D). At late anaphase I, sporocytes became flattened and elongated. They were

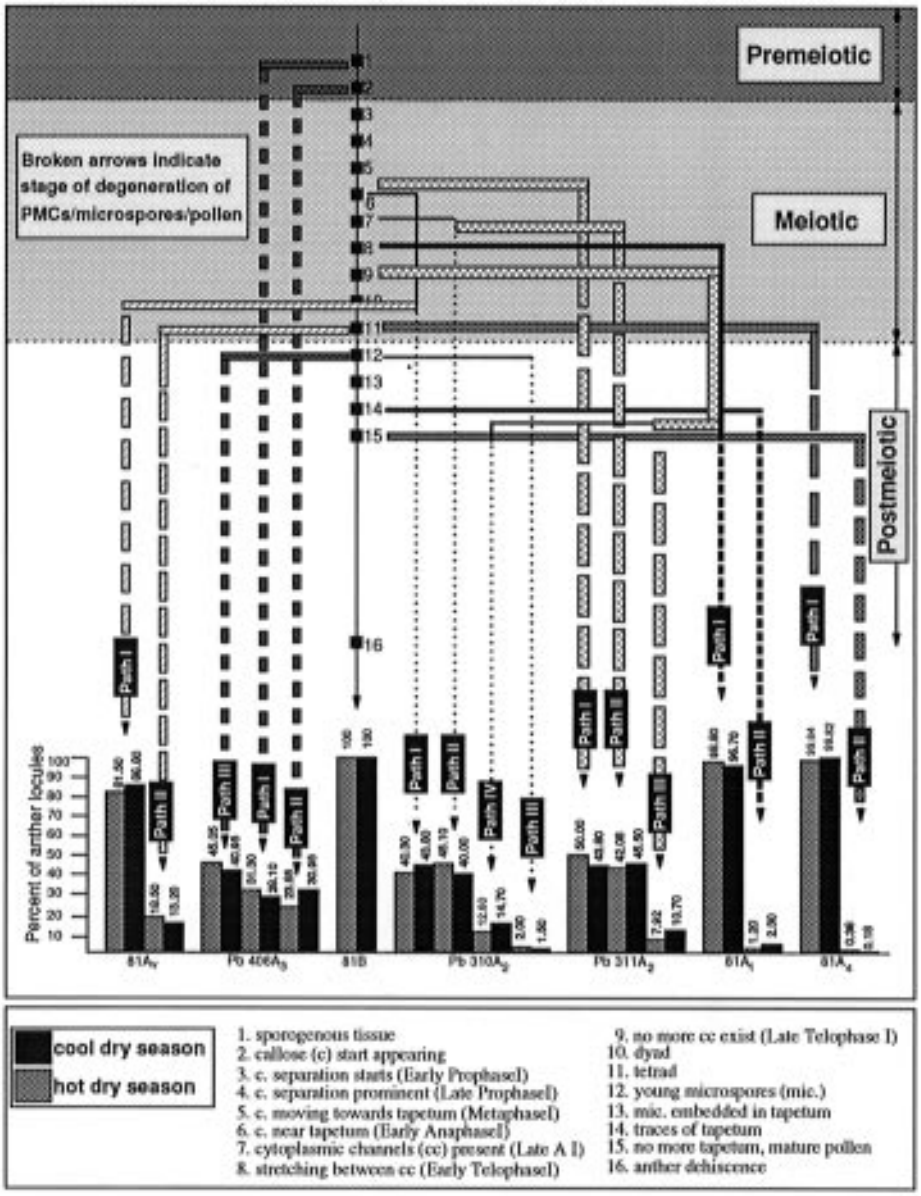

Figure 1. Comparison of microsporogenesis and PMC/microspore/pollen degeneration in pearl millet isonuclear lines.

interconnected by wide cytoplasmic channels (Figure 2E). At later stage, these cytoplasmic channels tend to break. Stretching of cytoplasmic channels was seen between the two adjacent sporocytes (Figure 2F), and subsequently, cytoplasmic continuities between sporocytes disappeared at telophase I (Figure 2G). Minute callose tips attached to sporocytes were seen even at the dyad stage and the anther middle layer was hardly detectable (Figure 2H). Callose breakdown occurred after the tetrad stage when young microspores were liberated (Figure 2I). Microspores were oriented in a ring along the densely stained tapetum (Figure 2J) and later on embedded in it (Figure 2K). Empty-looking pollen grains slowly filled with starch granules and the tapetum degenerated (Figures 2K–M). At this stage thickness of epidermis and endothecium was reduced. Well-filled pollen grains with starch granules and fully developed exine and intine were seen at the anther maturity (Figure 2M).

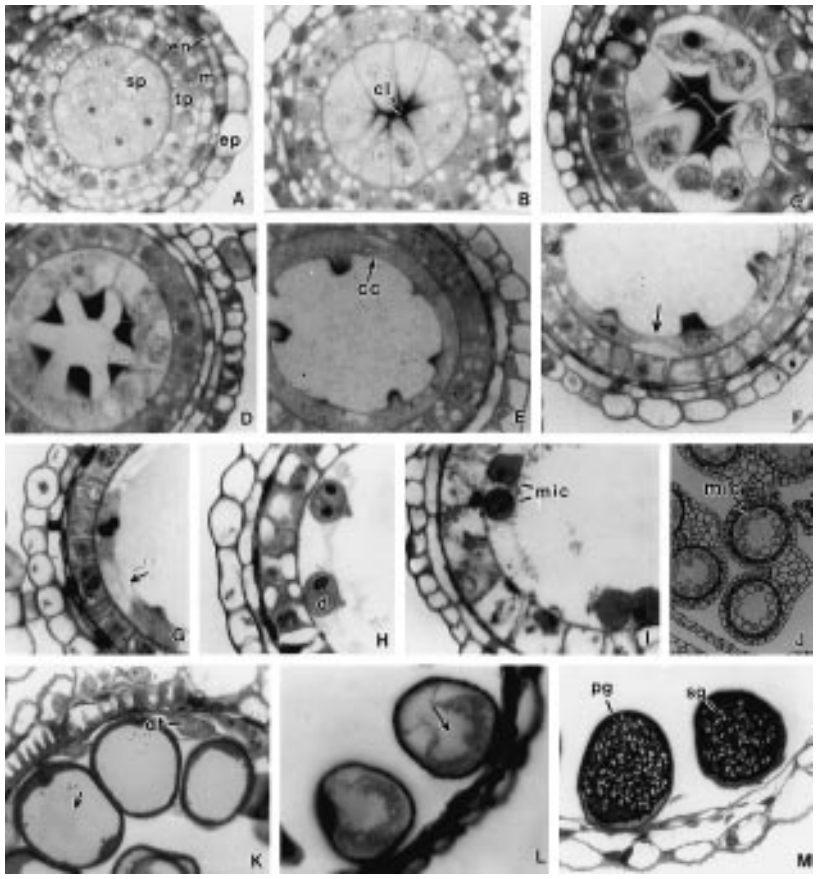

Figure 2A–M. Transverse sections of fertile anthers (81B) representing microsporogenesis from young sporogenous stage to pollen maturity. A – Young anther locule before callose deposition; B – Microsporocytes in early meiotic prophase with well developed callose; C – Central callose mass splitting along sporocyte walls; D – Separation and migration of sporocytes toward the tapetum. Note that each sporocyte carries a callose tip on its inner face; E – Anther locule showing microsporocytes at anaphase I; F – Cytoplasmic channels tend to break as stretching is seen (arrow) between adjacent sporocytes; G – No cytoplasmic continuities persist (arrow) between sporocytes that are at telophase I; H – Small callose tips attached to dyads; I – Young microspores immediately after liberation from tetrads; J – Developing uninucleate microspores in a ring along the densely stained tapetum; K – Apparent attachment of developing pollen grains (arrow) and the degenerating tapetum; L – Developing pollen grains (arrow) and remains of the degenerated tapetum; M – Mature pollen grains with many starch granules. Tapetum is no longer visible.
*Abbreviations used in figures:*cc – cytoplasmic channels, cf – fibrous callose, ct – callose tips, dm – degenerating/degenerated microspores, dt – degenerating tapetum, en – endothecium, ep – epidermis, ITS – intratapetal syncytium/periplasmodeum, m – middle layer, mic – microspores, n – nucleus/nuclei, pg – pollen grains, sg – sporogenous tissue, th – tapetal hypertrophy, tp – tapetum, vt – vacuolated tapetum.

Anther development and microsporogenesis in isonuclear A-lines

I. Premeiotic degeneration of PMCs/sporocytes

It was observed only in Pb 406A_3. About 30% of Pb 406A_3 locules examined showed degeneration of developing PMCs at stage 1 during the CDS and the HDS (Figure 1). Degeneration resulted due to anomalies in the tapetum or in developing PMCs themselves (Path I). In one kind of tapetal hypertrophy inner walls of tapetal cells appeared to dissolve and their cytoplasmic contents intermingled to form a periplasmodium attaining a balloon shape that almost covered the sporogenous tissues (Figure 3A). As a result, the anther locule collapsed very soon leading to death of developing PMCs. Such an anther typically had a thick epidermis, middle layer, endothecium, and very small compressed locular cavity containing debris of degenerated PMCs (Figure 3B). Another type of tapetal anomaly involved vacuolation of tapetal cells (Figure 3C) and disruption of tapetal cells due to imperfect differentiation of related tissues. These observations were similar to those of Sun & Ganders (1987) in Hawaiian *Bidens*, who also observed abnormal vacuolation

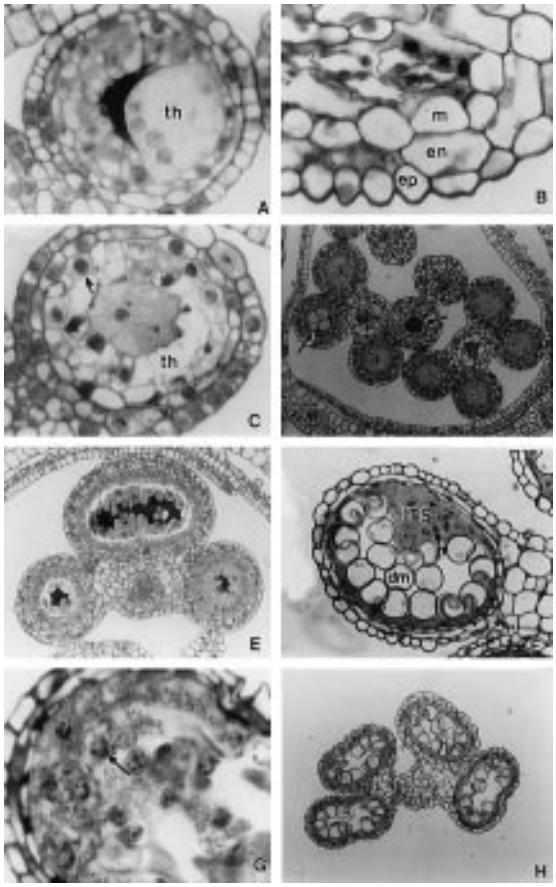

Figure 3A–H. Microsporogenesis in pearl millet A_3 cytoplasm male-sterile line Pb $406A_3$. *Figure 3 (A–D).* Transverse sections of Pb $406A_3$ anther locules exhibiting various tapetal irregularities compared to normal tapetal development in male-fertile line 81B (Figure 2A). A – Balloon shaped tapetal hypertrophy covering large area of locule. Floating tapetal nuclei can be seen; B – Collapsed locule with microsporocytes compressed between exceptionally thick anther wall layers; C – Unusual tapetum development with highly vacuolated lightly stained tapetal cells; D – Anthers within a floret showing normally developing locules (anther on right) and anomalies in two of the four locules (arrows) of a second anther (left). One of these anther locules has unstained giant microspores (left arrow) and the other has exceptionally darkly stained microspores; E – Trichambered (3 locules) anther; F – Anther locule at young microspore stage with plasmodial tapetum and degenerating microspores; G – Advanced stage compared to Figure 3F; H – Mature nondehiscent anther.

of tapetal cells during premeiotic period. The vacuolation increased rapidly to produce tapetal cells without cytoplasm and only nuclei were visible. As the highly vacuolated tapetal cells pressed upon the sporogenous cells, ultimately both the tapetum and sporogenous cells disorganized and disappeared. Another anomaly involved developing PMCs themselves where some anther locules had atypical giant PMCs (Figure 3D) or PMCs were unusually dark stained (Figure 3D). Locules containing giant cells had only 4–6 empty sporogenous cells. Such PMCs were not observed at later stages of anther development, suggesting their death at an early stage. At anther development stage 2, when callose started appearing near the locule center, degeneration occurred in about 31% of locules in the CDS and in about 24% of locules in the HDS (Figure 1). This degeneration also involved tapetal hypertrophy of different types (Path II). Tapetal cells enlarged unusually and masked the developing PMCs. Such locules could not be detected later suggesting their death at this premeiotic stage.

Two of $\approx$ 3000 Pb $406A_3$ anthers examined had an atypical trilobed structure instead of normal four lobes (Figure 3E). Two of the normal four lobes fused together to form this 3-lobed structure. Morphologically, all the four wall layers of the anther were normal except that the fused portion had none of the anther wall layers (Figure 3E). Such anthers were not found at later stages of anther development, suggesting their early degeneration.

II. Degeneration during meiosis

Microspore degeneration during meiosis was observed in Pb $310A_2$, Pb $311A_2$ and $81A_v$. These three CMS lines had identical developmental patterns up to the dyad stage, later, developing microspores degenerated in different ways in $81A_v$ and A_2-lines (Figure 1, Path I of each line).

(a) Pb $310A_2$ and Pb $311A_2$. Pb $310A_2$ followed four anther developmental paths and Pb $311A_2$ followed three. Two of the four anther developmental paths followed by Pb $310A_2$ showed degeneration of microsporocytes during meiosis (Figure 1). Some 40–44% of Pb $310A_2$ locules followed the path of 81B until early anaphase I. Thereafter, these followed a different developmental pattern (Path I). Disintegration of the cytoplasmic mass started at anaphase I. Callose remained attached to the sporocytes. The frequency of sporocytes with disintegrated cytoplasm abruptly increased at the dyad stage and callose breakdown also started (Figure 4A). Nuclei were densely stained and the degenerated cytoplasm also took more stain than the normal cytoplasm. Consequently, microspore degeneration occurred at the dyad stage.

Path II, which occurred in 40–45% of Pb $310A_2$ locules, was similar to 81B up to late anaphase I (Figure 1). Degeneration started immediately after this stage

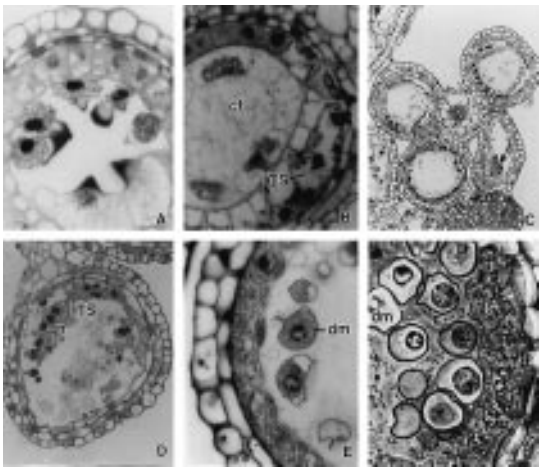

Figure 4A–F. Microsporogenesis in pearl millet A_2 cytoplasm CMS lines (Pb $310A_2$ and Pb $311A_2$). *Note: Anther developmental stages before this are the same as in Figures 2 (A–D). Thereafter, either the following path or the path of 81A*$_1$ *(Figure 6) was followed.* A – Anther locule at dyad stage; B – Anther developmental stage comparable to Figure 4A. Here callose breaks early to form fibrous strands; C – Anther showing disintegration of tapetum and microsporocytes. The cytoplasmic fluid floats freely inside the locule (arrow) or the tapetal cells enlarge due to breakdown of inner tapetal cell walls. The tapetum becomes vacuolated and microsporocytes degenerate completely leaving their cytoplasmic mass inside the locule (other three locules); D – Tapetal degeneration at the dyad stage. All three anther wall layers except the tapetum are prominent; E – Anther locule showing persistent typically fibrous tapetum and degenerating uninucleate microspores; F – Advanced stage of tapetal degeneration compared to Figure 4D.

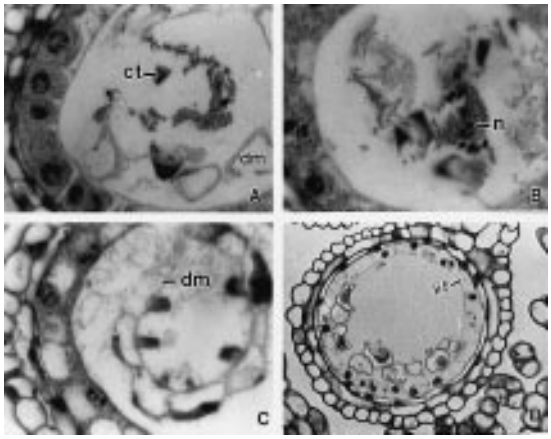

Figure 5A–D. Microsporogenesis in pearl millet *violaceum* cytoplasm CMS line $81A_v$ = ICMA 88001. *Note: Microsporogenesis is same as that of A*$_2$ *cytoplasm lines up to Figure 4A, thereafter, the following stages were observed.* A – Microsporocytes degenerate at the dyad stage and callose breakdown occurs; B – As above (Figure 5A) but at an advanced stage. C – Comparable to Figure 5A but callose tips remain attached to microsporocytes; D – Mature anther locule with degenerated uninucleate microspores and intact and highly vacuolated tapetum.

(Figure 1, stage 7). It resulted due to degeneration of the cytoplasmic mass and sporocyte walls (Figure 4B). Callose breakdown occurred in the form of fibrous strands scattered throughout the locule. Almost simultaneously, interconnecting tapetal cell walls started dissociating. Cytoplasmic fluid and nuclei of tapetal cells floated together (Figure 4B) and the tapetum became highly vacuolated. Subsequently, in some anther locules either sporocytes and the tapetum degeneration occurred simultaneously or tapetum degeneration was followed by that of sporocytes (Figure 4C).

Two of the three anther developmental paths observed in Pb $311A_2$ were similar to those of Pb $310A_2$ Path I and Path II described above, but their frequencies of occurrence were slightly different (Figure 1).

(b) ICMA 88001 (= 81A$_v$*).* Pollen abortion in $81A_v$ resulted from one of the following phenomena: Firstly, anther development was similar to Pb $310A_2$ up to the dyad stage (Figure 1). Later on, degeneration occurred in different ways (c.f. Figure 4A). This occurred in 81–87% of the $81A_v$ locules (Path I). Broken callose tips from sporocytes remained intact and were seen with the cytoplasmic mass and nuclei released from sporocytes after the breakdown of their walls (Figure 5A). Later, debris of callose, nuclei, cytoplasmic mass and disintegrated walls of sporocytes gathered in the locule center (Figure 5B). Unlike in $81A_1$, callose and microspore degeneration occurred almost simultaneously indicating early callase activity coupled with some other biochemical events that led to dissolution of the sporocyte walls.

The second type of degeneration in $81A_v$ occurred in 13–18% of anther locules (Path II). Sporocytes with the callose tips attached migrated towards the locule interior. Simultaneously, sporocytes' walls started breaking resulting in release of the cytoplasmic fluid (Figure 5C). Big vacuoles were present in the tapetum in this second type of degeneration that were absent in the first. In this case, microspore degeneration occurred not because of callose breakdown, but apparently as a result of tapetum vacuolation and loss of contact between developing microsporocytes and tapetum that led to sporocytes starvation (Figure 5C). In addition, the tapetum thickness continued to increase towards anther maturity and persisted longer than 81B.

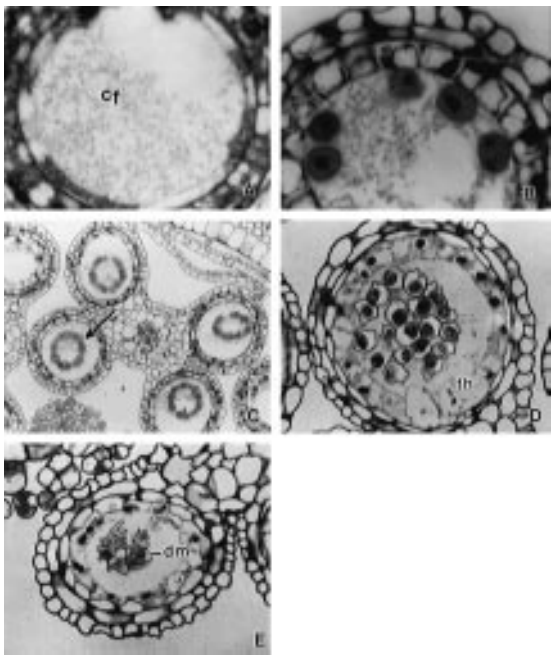

Figure 6A–E. Microsporogenesis in pearl millet A_1 cytoplasm CMS line $81A_1$. *Note: Anther development is similar to that of 81B (normal) up to Figure 2F, then the following anther developmental stages were observed in* $81A_1$. A – Callose breakdown occurs and fibrous strands are formed; B – Late dyad/early tetrad stage with thick, highly vacuolated tapetum; C – Microspores form a ring (arrow) and migrate toward the locule interior (contrary to 81B, Figure 2J); D – Degenerating microspores containing contracted cytoplasmic mass. Note the ocurrence of tapetal hypertrophy; E – Anther locule showing completely degenerated microspores and persistent tapetum.

III. Postmeiotic degeneration of microspores/pollen grains

Postmeiotic degeneration of microspores was observed in all isonuclear A-lines. All the anther locules of $81A_1$ and $81A_4$ followed postmeiotic degeneration. In Pb $406A_3$, it occurred in 41–45% of locules (Figure 1, Path III of Pb $406A_3$), whereas, in all other A-lines it was observed in low proportion of anther locules. The process of anther development/microsporogenesis of each line has been presented below.

(a) $81A_1$. Two anther developmental paths were observed in $81A_1$. Path I occurred in 97–99% of the locules that was similar to that of 81B up to early telophase I. Subsequently callose breakdown occurred forming fibrous strands that spread throughout the locular cavity (Figure 6A). Tapetum became thick and highly vacuolated at the late dyad stage (Figure 6B). Dyads and young microspores remained adhered to the tapetum as in 81B, but later, microspores formed a ring and migrated towards the locule interior (compare Figures 2J and 6C). Tapetum thickness and vacuolation continued to increase. The anther middle layer, hardly detectable at the dyad and the tetrad stages, reappeared and became prominent. Some microspores became binucleate by this stage. In advanced stages of anther development, cytoplasmic contraction (of microspores) and tapetal hypertrophy occurred and microspores started shrinking (Figure 6D). Ultimately, microspores degenerated completely and formed cluster in the locule center, the tapetum still persisted (Figure 6E).

The callose behavior in fertile anthers (of 81B) was normal and similar to the observations of Warmke & Overman (1972) in male-fertile anthers of sorghum. They observed the central callose mass to split into sectors along planes of the original microsporocyte walls and form a covering effectively isolating the microsporocytes and young microspores. This special wall later dissolved to release microspores from the tetrads. These microspores contacted the tapetum and were nourished to develop into healthy and fertile pollen grains. They also observed significant differences between male-sterile and male-fertile sorghum anthers for callose formation and callase activity. Two major differences between $81A_1$ and 81B were: (1) early callose breakdown in $81A_1$ (compare Figures 2I and 6A), and (2) migration of young microspores away from the tapetum i.e. towards the locule interior that might have resulted in starvation of young microspores because of loss of close association of developing microspores and the tapetum as also observed by Warmke & Overman (1972) in sorghum. Thus, these two anomalies appear to contribute to pollen sterility in $81A_1$. Overman & Warmke (1972) also observed that untimely callase activity leading to late or early breakdown of callose disturbs microsporogenesis and leads to male sterility.

A second type of pollen degeneration in $81A_1$, observed only in 1–2% of the locules (Path II) had anther development similar to 81B until stage 14 (Figure 2K). Thereafter, pollen grains started collapsing. Such anthers did not dehisce and contained remnants of degenerated tapetum and pollen grains.

(b) Pb $310A_2$ *and Pb* $311A_2$. Two of the four paths followed in Pb $310A_2$ (Figure 1) showed postmeiotic degeneration of microspores at young microspore stage in 1–2% of locules (Figure 1, Path III of Pb $310A_2$) or near pollen maturity in 13–15% of locules (Path IV). In Path III, anther development was simi-

lar to 81B till liberation of microspores from tetrads. Thereafter, tapetal cytoplasm typically turned fibrous and microspores degenerated at the uninucleate stage (Figure 4E) perhaps due to the inability of the fibrous tapetum to supply nutrition to developing microspores. Path IV was similar to 81B up to late telophase I, then joined that of $81A_1$, i.e. callose breakdown at telophase I followed by loss of contact between microspores and the tapetum resulting in microspore degeneration. In Pb $311A_2$, 8–10% of locules followed developmental Path III. Thus, anther development of Pb $310A_2$ and Pb $311A_2$ followed four different paths, each with its own cause of microspore degeneration.

(c) Pb 406A$_3$. Anther/pollen development in 41–45% of Pb $406A_3$ locules proceeded normally up to release of microspores from the tetrads. Thereafter, degeneration occurred due to the formation of an intratapetal syncytium. Tapetal cell walls facing the sporocytes remained intact and bulged out to cover the locule interior and surrounded the microspores (Figure 3F). Ultimately, locules were completely filled with periplasmodium and microspores died (Figure 3G). Overman & Warmke (1972) also observed as many as 50% of anthers in male-sterile sorghum were affected by an intratapetal syncytium. A few A_3 cytoplasm anthers were observed having darkly stained and persistent tapetum, and compressed empty microspores at maturity (Figure 3H).

(d)81A$_m$ *= 81A*$_4$ Most $81A_4$ locules (> 99%) followed an identical anther developmental pattern (Path I). The second pattern (Path II) occurred very rarely (< 0.5% of locules). Path I was similar to 81B up to the tetrad stage (Figure 1). Thereafter, young microspores scattered inside the locular cavity, became oriented in a circle along the inner tapetal wall (Figure 7A). Microspores then embedded in the tapetum (Figure 7B) and both (microspores and the tapetum) degenerated simultaneously (Figure 7C). Ultimately, the contact between the tapetum and microspores was lost, and only microspore walls (collapsed microspores) and disintegrated tapetum were present in the locular cavity (Figure 7D). Path II of $81A_4$ could not be distinguished from 81B till formation of mature pollen grains. Pollen degeneration then occurred suddenly and anthers contained traces of tapetum and degenerated pollen grains.

The general belief that degenerating tapetal cells nourish developing microspores is difficult to explain male sterility of $81A_4$ as no observable tapetal abnormality was noticed in male sterile $81A_4$. It therefore,

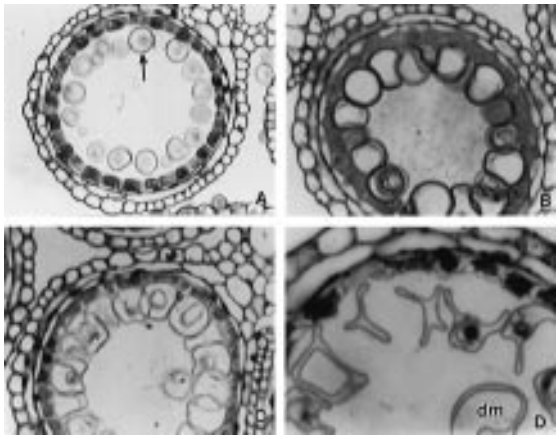

Figure 7A–D. Microsporogenesis in pearl millet A_4 cytoplasm CMS line $8A1_4$. *Note: Microsporogenesis in 81A*$_4$ *is similar to that of 81B in Figures 2A–2I. Thereafter, the following anther developmental stages were observed.* A – Microspores attached to the tapetum are arranged along the inner tapetal wall. Tapetum is densely stained and individual tapetal cells can be seen; B – Tapetum and microspores start degenerating simultaneously; C – Tapetum and microspore degeneration proceeds; D – Contact between completely degenerated microspores (dm) and the tapetum is lost. The tapetum is reduced to an irregular mass.

appears that abnormality in some process other than tapetal degeneration exists in $81A_4$. Similar observations on $81A_1$ (Figure 1, Path II of $81A_1$) indicated that factors within the pollen grains were responsible for pollen abortion in these two A-lines. Similar situations (normal tapetum degeneration) were observed by Balarami Reddy & Reddi (1974) in pearl millet A_1 cytoplasm male-sterile line 628A and Lee et al. (1980) in S-cytoplasm male-sterile maize (*Zea mays* L.). These investigations and similar studies undertaken by earlier researchers (Webster & Singh, 1964) suggested that the endothecium can also play a major role in pollen fertility, as anthers of male-fertile lines possess a very thin endothecium near maturity. No other observable reason could be assigned for pollen abortion in $81A_4$ except that it had very thick endothecium (7–8 μ in $81A_4$ compared to 2 μ in 81B) even at anther maturity. Other unknown events may also be involved that lead to degeneration of developing pollen grains in $81A_4$.

(e) ICMA 88001 (= 81A$_v$*).* From the precallose to tetrad stage, all the tissues of the $81A_v$ anthers appeared normal and were indistinguishable from those in fertile maintainer line 81B. Differences in the tapetum appeared at later stages. The persistent and highly vacuolated tapetum at maturity, with very light-

Table 1. Stage(s) of tapetum degeneration in isonuclear A-lines of pearl millet

A-line	Stage of tapetum degeneration		
	Premeiotic degeneration	Degeneration during meiosis	Postmeiotic degeneration
$81A_1$	–	–	Yes
Pb $310A_2$	–	Yes	Yes
Pb $311A_2$	–	Yes	Yes
Pb $406A_3$	Yes	–	Yes
$81A_4$	–	–	Yes
$81A_v$	–	Yes	Yes

ly stained cytoplasm and darkly stained nuclei (Figure 5D) could be assigned to male sterility in $81A_v$. Most of the microspores were uninucleate, shrunken and had contracted cytoplasm at anther maturity. About 13% (CDS) to 19% (HDS) of A_v locules followed this path (Figure 1, Path II).

Developmental changes in tapetum and endothecium
The tapetum attained its maximum thickness at the tetrad stage in most isonuclear lines. In 81B also, tapetum thickness was maximum (15.2 μ) at the tetrad stage (Figure 2I). Thereafter, it thinned drastically and nearly disappeared at anther dehiscence (Figure 2M). Almost similar developmental pattern was observed in $81A_4$. In $81A_1$, tapetum thickness started decreasing after the tetrad stage (15.0 μ) in the CDS or at young microspore stage (15.3 μ) in the HDS, but the vacuolated tapetum was still conspicuous (13–14 μ) at pollen maturity (Figure 6E). Tapetum thickness continued to increase after the tetrad stage in male-sterile lines having the A_2 and A_3 cytoplasm. Maximum tapetum thickness was attained either at the young microspore stage (12–15 μ) or at pollen formation (17–18 μ) i.e. the tapetum persisted till anther maturity, but tapetal cells lost their identity because of ITS formation. The most extreme case of ITS was observed in Pb $406A_3$ as tapetal material dispersed completely in the locular cavity (Figure 3G). On the other hand, the situation was not so bad in A_2-lines since the tapetum retained its shape to some extent even after ITS formation. These observations indicate that postmeiotic tapetal degeneration was a common phenomenon in most of the A-lines (Table 1). The endothecium was well developed in all seven isonuclear lines at early stages of anther development. In 81B the endothecium attained its maximum thickness at the dyad stage (4.2 μ) then decreased in thickness as microspores matured, facilitating anther dehiscence. It has been shown that a thick endothecium is gradually attenuated to facilitate dehiscence in male-fertile sorghum (Webster & Singh, 1964) and pearl millet (Balarami Reddy & Reddi, 1970, 1974) but in male sterile material no such phenomenon was previously observed. Our results in 81B (fertile), $81A_1$ and 81_4 were in agreement with these findings. In $81A_1$ and 81_4 endothecium thickness increased rapidly (7–9 μ) as anthers matured contributing to nondehiscence of anthers, whereas, in Pb $406A_3$ and Pb $311A_2$, endothecium thickness declined near maturity after the dyad/tetrad stage. These latter two lines (Pb $406A_3$ and Pb $311A_2$) had higher pollen fertility than the other A-lines in which the endothecium thickness was thicker (Chhabra, 1995) in accordance with the findings of Pritchard & Hutton (1972) in *Phaseolus atropurpureus*.

Conclusions

Each cytoplasm included in this study had its own effect on microsporogenesis. The different cytologies of A_1, A_2, A_3, A_4 and A_v pollen abortion suggest that fundamentally different mechanisms are involved. There are several events that determine cytoplasmic male sterility. For example, meiotic anomalies (Chhabra, 1995), tapetal hypertrophy, persistence of tapetum, endothecium thickness, and anomalies in callose behavior etc. These events differ with cytoplasm and hence it is not possible to identify a particular event as a common cause of male sterility in all. This was also advocated by Laser & Larsten (1972).

These studies clearly indicated that anther/pollen development is more irregular in A_3 CMS line Pb $406A_3$. In $81A_4$ and $81A_1$ > 95% of anther locules followed single developmental paths leading to pollen abortion. In other A-lines many developmental paths were observed within a line and pollen degeneration occurred at various stages. This probably contributes to instability of male sterility in the A_2 and A_3 systems and stability of male sterility in the A_1 and A_4 systems. Rai (1993) evaluated the effect of five different CMS sources (A_1, A_2, A_3, A_4 and A_v) on pollen shedder frequency and selfed seed-set in hot dry and rainy seasons and reported similar findings, concluding that A-lines with the A_2 and A_3 cytoplasms, in addition to having more pollen shedders, also had a much higher degree of self seed-set on apparently male-sterile plants than did $81A_1$, $81A_4$, and $81A_v$. The present study supports the conclusions of Rai (1994), that from the view point

of sterility maintenance, the A_1, and A_4 CMS systems are better than the A_v, A_2 and A_3 systems, at least in the nuclear background of 81B.

Acknowledgements

The senior author is thankful to the Council of Scientific and Industrial Research (CSIR), Government of India, for the award of a Senior Research Fellowship (SRF) and to ICRISAT Asia Center (IAC), Patancheru, Andhra Pradesh, India for the grant of Research Scholarship to conduct the PhD research work, a part of which is published in this article.

References

Aken'Ova, M.E., 1985. Confirmation of a new source of cytoplasmic-genic male-sterility in bulrush millet [*Pennisetum americanum* (L.) Leeke]. Euphytica 34: 669–672.

Anand Kumar, D.J. Andrews, R.P. Jain & S.D. Singh, 1984. ICMA-1 and ICMB-1 pearl millet parental lines with A1 cytoplasmic-genic male sterility system. Crop Sci 24: 832.

Appadurai, R., T.S. Raveendran & C. Nagarajan, 1982. A new male-sterility system in pearlmillet. Indian J Agric Sci 52: 832–834.

Balarami Reddy, B. & M.V. Reddi, 1970. Studies on the breakdown of male sterility and other related aspects in certain cytoplasmic male-sterile lines of pearl millet (*Pennisetum typhoides Stapf and Hubb*). Andhra Agric J 17: 173–180.

Balarami Reddy, B. & M.V. Reddi, 1974. Cytohistological studies on certain male sterile lines of pearl millet (*Pennisetum typhoides* S. & H.). Cytologia 39: 585–589.

Burton, G.W., 1958. Cytoplasmic male-sterility in pearl millet (*Pennisetum glaucum*) (L.) R Br Agron J 50: 230.

Burton, G.W. & D.S. Athwal, 1967. Two additional sources of cytoplasmic male sterility in pearl millet and their relationship to Tift 23A. Crop Sci 7: 209–211.

Chhabra, A.K., 1995. Molecular characterization of cytoplasmic-nuclear male sterility (CMS) sources and tall/dwarf near-isogenic lines in pearl millet. PhD thesis submitted to CCS Haryana Agricultural University, Hisar 125 004, Haryana, India.

Hanna, W.W., 1989. Characteristics and stability of a new cytoplasmic-nuclear male-sterile source in pearl millet. Crop Sci 29: 1457–1459.

Laser, K.D. & N.R. Larsten, 1972. Anatomy and cytology of microsporogenesis in cytoplasmic male sterile angiosperms. Bot Rev 38: 425–454.

Lee, S.L.J., V.E. Gracen & E.D. Earle, 1979. The cytology of pollen abortion in C-cytoplasmic male-sterile corn anthers. Amer J Bot 66: 656–667.

Lee, S.L.J., E.D. Earle & V.E. Gracen, 1980. The cytology of pollen abortion in S cytoplasmic male-sterile corn anthers. Amer J Bot 67: 237–245.

Marchais, L. & J. Pernes, 1985. Genetic divergence between wild and cultivated pearl millets (*Pennisetum typhoides*). I. Male sterility. Z. Pflanzenzüchtg 95: 103–112.

Overman, M.A. & H.E. Warmke, 1972. Cytoplasmic male sterility in sorghum. II. Tapetal behaviour in fertile and sterile anthers. J Hered 63: 227–234.

Pritchard, A.J. & E.M. Hutton, 1972. Anther and pollen development in male-sterile *Phaseolus atropurpureus*. J Hered 63: 280–282.

Rai, K.N., 1994. Selfed seed-set in male-sterile lines of pearl millet. In: Cereals Program Annual Report (1993). Cereals Program, International Crops Research Institute for the Semi-Arid Tropics, Paanchuru, India, pp. 84–87.

Rai, K.N., 1995. A new cytoplasmic-nuclear male sterility system in pearl millet. Plant Breeding 114: 445–447.

Rai, K.N. & C.T. Hash, 1990. Fertility restoration in male sterile × maintainer hybrids of pearl millet. Crop Sci 30: 889–892.

Rajeshwari, R., S. Sivaramakrishnan, R.L. Smith & N.C. Subrahmanyam, 1994. RFLP analysis of mitochondrial DNA from cytoplasmic male-sterile lines of pearl millet. Theor Appl Genet 88: 441–448.

Sharma, Y.P., 1978. Investigation into the causes of male sterility in pearl-millet (*Pennisetum glaucum* Linn.) R. Br. Bangladesh J Bot 7(2): 6–9.

Singh, S.P. & Y.P. Sharma, 1963. Preliminary observations on the breeding of *Pennisetum* at B.R. College, Bichpuri, Agra, India. Sorghum Newsletter 6: 26–28.

Sivaramakrishnan, S., R. Rajeshwari, N.C. Subrahmanyam, R.L. Smith, V. Sujata & K.N. Rai, 1993. Molecular characterization of cytoplasmic male sterile lines of pearl millet. In: Cereals Program Annual Report (1992). Cereals Program, International Crops Research Institute for the Semi-Arid Tropics, Patancheru, India, pp. 83–85.

Smith, R.L. & M.K.U. Chowdhury, 1989. Mitochondrial DNA polymorphism in male-sterile and fertile cytoplasms of pearl millet. Crop Sci 29: 809–814.

Smith, R.L. & M.K.U. Chowdhury, 1991. Characterization of pearl millet mitochondrial DNA fragments rearranged by reversion from cytoplasmic male-sterility to fertility. Theor Appl Genet 81: 793–799.

Smith, R.L., M.K.U. Chowdhury & D.R. Pring, 1987. Mitochondrial DNA rearrangements in *Pennisetum* associated with reversion from cytoplasmic male sterility to fertility. Plant Mol Biol 9: 277–286.

Spurr, A.R., 1969. A low viscosity epoxy resin embedding medium for electronmicroscopy. J Ultrastruct Res 26: 31.

Sujata, V., S. Sivaramakrishnan, K.N. Rai & K. Seetha, 1994. A new source of cytoplasmic male sterility in pearl millet: RFLP analysis of mitochondrial DNA. Genome 37: 482–486.

Sun, M. & F.R. Ganders, 1987. Microsporogenesis in male-sterile and hermaphroditic plants of nine gynodioecious taxa of Hawaiian *Bidens* (Asteraceae). Amer J Bot 74: 209–217.

Virk, D.S. & B.K. Mangat, 1987. Substitution of CMS 81B genome into A_2 cytoplasm. Millet Newslett 6: 6.

Virk, D.S. & B.K. Mangat, 1988. Substitution of 81B genome into A_3 cytoplasm. Millet Newslett 7: 3.

Virk, D.S. & B.K. Mangat, 1989. Alloplasmic lines of L67A in pearl millet. Millets Newslett 8: 3.

Virk, D.S., B.K. Mangat & K.S. Gill, 1990. Pb 310A_2 and Pb 406A_3, isonuclear male sterile lines of pearl millet. J Res Punjab Agric Univ, Ludhiana 27: 359.

Warmke, H.E. & M.A. Overman, 1972. Cytoplasmic male sterility in sorghum. I. Callose behaviour in fertile and sterile anthers. J Hered 63: 102–108.

Webster, O.J. & S.P. Singh, 1964. Breeding behaviour and histological structure of a non-dehiscent anther character in *Sorghum vulgare* Pers. Crop Sci 4: 656–658.